


2003

Fenske-Hall Approximate Molecular Orbital Analysis of the Chelating Carbene Complex $\eta^5\text{-Cp}'(\text{CO})\text{Mn}\{\text{C}(\text{OEt})\text{CH}_2\text{PPh}_2\}$

John P. Graham
Arkansas Tech University

Follow this and additional works at: <https://scholarworks.uark.edu/jaas>

 Part of the [Other Chemistry Commons](#)

Recommended Citation

Graham, John P. (2003) "Fenske-Hall Approximate Molecular Orbital Analysis of the Chelating Carbene Complex $\eta^5\text{-Cp}'(\text{CO})\text{Mn}\{\text{C}(\text{OEt})\text{CH}_2\text{PPh}_2\}$," *Journal of the Arkansas Academy of Science*: Vol. 57, Article 9.

Available at: <https://scholarworks.uark.edu/jaas/vol57/iss1/9>

This article is available for use under the Creative Commons license: Attribution-NoDerivatives 4.0 International (CC BY-ND 4.0). Users are able to read, download, copy, print, distribute, search, link to the full texts of these articles, or use them for any other lawful purpose, without asking prior permission from the publisher or the author.

This Article is brought to you for free and open access by ScholarWorks@UARK. It has been accepted for inclusion in *Journal of the Arkansas Academy of Science* by an authorized editor of ScholarWorks@UARK. For more information, please contact scholar@uark.edu, uarepos@uark.edu.

Fenske-Hall Approximate Molecular Orbital Analysis of the Chelating Carbene Complex $\eta^5\text{-Cp}'(\text{CO})\text{Mn}\{\text{C}(\text{OEt})\text{CH}_2\text{PPh}_2\}$

John P. Graham
Department of Physical Science
Arkansas Tech University
Russellville, AR 72801

Abstract

The novel three legged piano stool chelating carbene complex, $\text{Cp}'(\text{CO})\text{Mn}\{\text{C}(\text{OEt})\text{CH}_2\text{PPh}_2\}$, 1, exhibits interesting structural, spectroscopic and electrochemical properties. It also readily undergoes reaction with CO to produce the three-legged piano stool complex $\text{Cp}'(\text{CO})_2\{\text{PPh}_2\text{C}(\text{OEt})=\text{CH}_2\}$, 2. This is in contrast to the analogous non-chelating complex $\text{Cp}(\text{CO})(\text{PPh}_3)\text{Mn}\{\text{C}(\text{OMe})\text{CH}_2\text{CH}_3\}$, 3, which does not react with CO. This paper discusses the results of Fenske-Hall approximate molecular orbital calculations on model complexes for 1 and 3. The differences in spectroscopic and electrochemical properties are explained using molecular orbital analysis. Possible reasons for the enhanced reactivity of 1 are also presented.

Introduction

Transition metal carbene complexes have been the subject of extensive study for many years (Schrock, 2001; Frenking and Froelich, 2000). Fenske and Kostic (1982) and Schilling et al. (1979) described the conformational preferences of the carbene ligand in transitional metal-carbene complexes: For carbene complexes of the type $\text{CpM}(\text{L})_2(\text{CB})$ ($\text{L} = \pi$ acceptor ligand such as CO, CB = carbene), the orientation of the carbene plane relative to the ligands L has been shown to have considerable effect on the electronic structure. The two extreme orientations of interest are illustrated in Fig. 1. It has been shown that the vertical orientation is more stable than the horizontal orientation, based on energetic and orbital overlap arguments.

Complexes of the form $\text{CpMLL}'(\text{CB})$, where L and L' differ considerably in π acceptor ability, have been shown to adopt an orientation in which the plane of the carbene ligand is parallel to the M-L vector, where L is the better π

accepting ligand (Kiel et al., 1980). The two extreme orientations labeled 'parallel' and 'perpendicular' are illustrated in Fig. 2.

The recently synthesized complexes 1 and 3 exhibit different carbene orientations (Lugan, pers. comm.): Complex 3 exhibits the standard conformation with the carbonyl ligand parallel to the plane of the carbene ligand. Complex 1 is forced, by the chelating nature of the carbene, to adopt the normally unfavorable orientation with the CO perpendicular to the carbene plane. The structure of complex 1 is represented by a ball and stick description in Fig. 3. It is noteworthy that the C1-C-P angle in the chelating ligand is unusually small (89°) and that the C-P distance indicated by the dashed line is quite short (2.36 \AA). It has been observed that complex 1 exhibits enhanced reactivity, a higher oxidation potential, and lower CO stretching frequency than complex 3 (Lugan, pers. comm.). These differences in observed properties could arise from strain within the chelating ligand of 1 or from the unfavored orientation of the chelating ligand with respect to CO. The

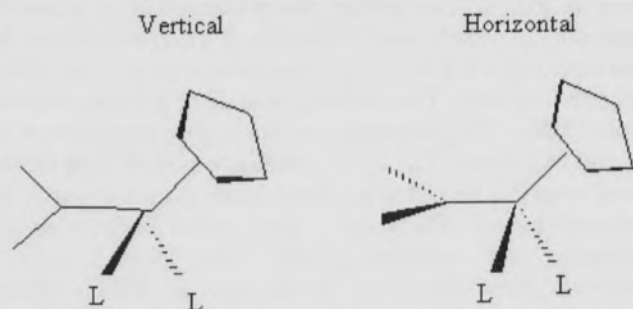


Fig. 1. Extreme orientations of the complex $\text{CpM}(\text{L})_2\text{CB}$, $\text{L} = \text{strong } \pi$ acid ligand.

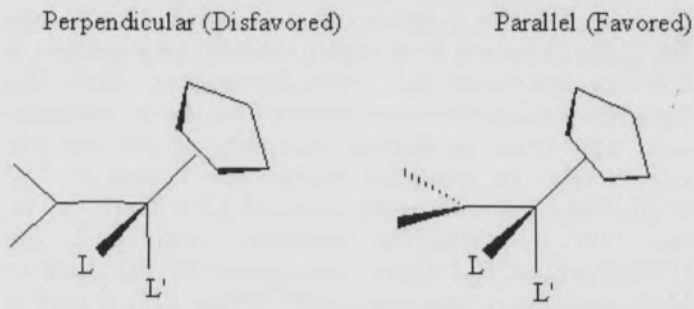


Fig. 2. Extreme orientations of the complex $\text{CpMLL}'\text{CB}$, where L and L' differ considerably in π acidity.

Fenske-Hall Approximate Molecular Orbital Analysis of the Chelating Carbene Complex
 $\eta^5\text{-Cp}'(\text{CO})\text{Mn}\{\text{C}(\text{OEt})\text{CH}_2\text{PPh}_2\}$

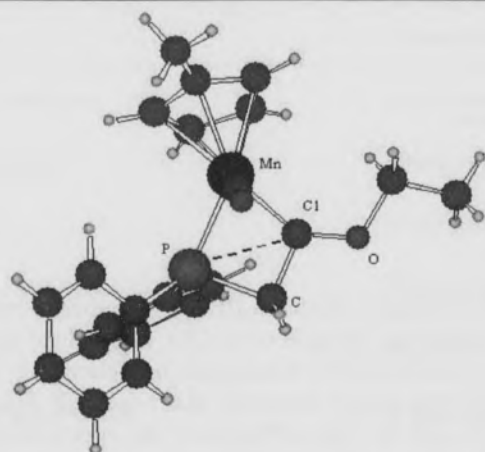


Fig. 3. A ball-and-stick representation of complex 1. The dashed line between P and C1 indicates a weak interaction.

origin of the observed differences between complexes 1 and 3 will be the main focus of this paper.

To simplify the calculations, model complexes have been used. The model for complex 1 is $\text{Cp}(\text{CO})\text{Mn}\{\text{C}(\text{OMe})\text{CH}_2\text{PH}_2\}$ and labelled 1a. The model for complex 3 is $\text{Cp}(\text{CO})\text{Mn}(\text{C}(\text{OMe})\text{Me})\text{PH}_3$. To help study the effect of carbene orientation without the necessity to consider other factors, two structures are considered; the observed 'parallel' orientation, 3a, and the unfavorable 'perpendicular' orientation, 3b. We will initially compare model complex 3a with the unfavorable model isomer 3b. Comparisons will then be made between 3b and the model complex 1a.

Methods

The Fenske-Hall approximate molecular orbital method was used for all calculations (Hall and Fenske, 1972). All atomic basis functions were generated by a least-squares fit of Slater-type orbitals to the atomic orbitals from Herman-Skillman atomic calculations (Bursten et al., 1978). Contracted double ζ representations were used for the Mn 3d, C 2p, O 2p and P 3p atomic orbitals. An exponent of 1.16 was used for the H 1s AO's (Hehre et al., 1969). The basis functions for Mn were derived from the +1 oxidation state with fixed 4s and 4p exponents of 2.0 and 1.8, respectively. In modeling complexes 1 and 3, Cp' ($\text{C}_5\text{H}_4\text{CH}_3$) was replaced by Cp (C_5H_5), Ph (C_6H_5) by H, and OEt by OMe. In modeling complex 2, the $\{\text{PPh}_2\text{C}(\text{OEt})=\text{CH}_2\}$ ligand was replaced by PH_3 , and L-Mn-L angles were idealized to 90° . Where PH_3 is used to model PPh_3 , a H-P-H angle of 102° is employed (Clayton, 1989). The 3σ and 6σ orbitals of CO and all Cp orbitals below the lowest occupied π orbital and above the highest unoccupied π orbital were deleted from the set of variational

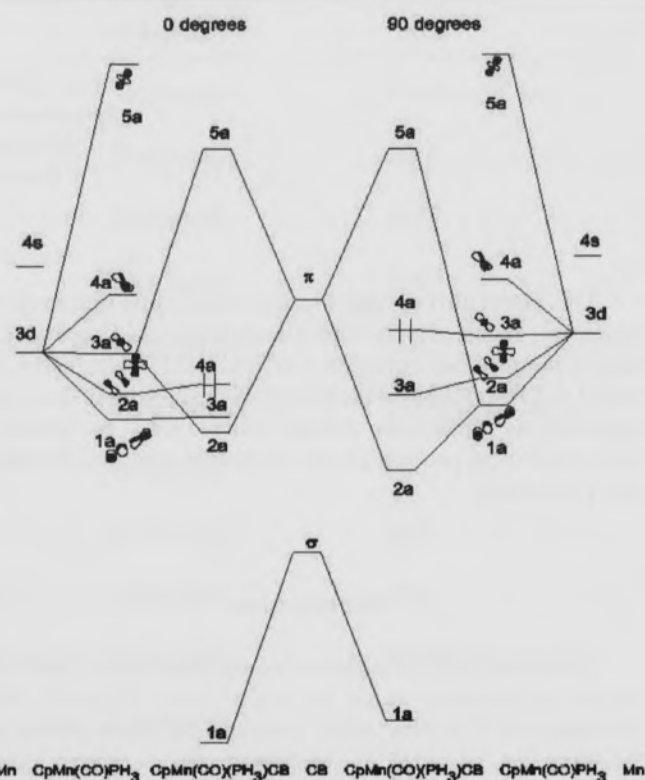


Fig. 4. A molecular orbital diagram complexes 3a and 3b.

orbitals (Lichtenberger and Fenske, 1976). The carbene plane - CO vector angles were idealized at 90° or 0° where appropriate. All other bond distances and angles were preserved as in the crystal structures (Lugan, N., Laboratoire de Chimie de Coordination, Toulouse, France. pers. comm.)

Results and Discussion

Comparison of model complexes 3a and 3b.--A molecular orbital description of complexes 3a and 3b is given in Fig. 4. The results are presented in a fragment approach, in which each molecule is represented by the interaction of a $\text{CpMn}(\text{CO})_2$ fragment with a $\text{CMe}(\text{OMe})$ carbene fragment. The frontier orbitals of primary interest of the $\text{CpMn}(\text{CO})_2$ fragment are the largely metal based 1a, 2a, and 3a orbitals. The local coordinate system used for the metal center is such that the local z axis points towards the carbonyl ligand. The local y axis points in-between the phosphine and carbene ligands. The local x axis is perpendicular to the plane of the page. In this coordinate system, the composition of the metal based frontier orbitals of $\text{CpMn}(\text{CO})_2$ are as follows: The orbitals 1a and 2a are the $\text{Mn } d_{xz} - \text{CO}2\pi_x$ and $\text{Mn } d_{yz} - \text{CO}2\pi_y$ bonding molecular orbitals respectively; orbital 3a is an essentially

John P. Graham

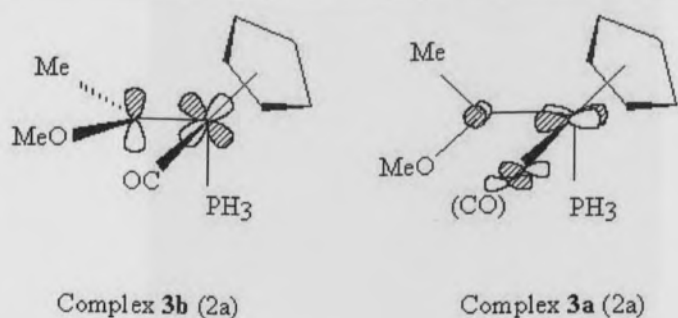


Fig. 5. The carbene π^* - $\text{CpMn}(\text{CO})(\text{PH}_3)$ interactions in complexes 3a and 3b.

non-bonding Mn $d_{x^2-y^2}$ based orbital. The principal frontier orbitals of the carbene ligand are those labeled σ and π^* . The carbene σ orbital is essentially a lone pair of electrons localized largely on the carbene C1 (the C bound to Mn) atom. The π^* orbital is a virtual orbital perpendicular to the plane of the carbene ligand and is antibonding between C1 and O, mostly localized on C1. In complex 3a, the Mn $d_{x^2-y^2}$ based non-bonding HOMO (Highest Occupied Molecular Orbital) of $\text{CpMn}(\text{CO})_2$ donates electron density to the π^* orbital of the carbene ligand. The resultant stabilized molecular orbital 2a has considerable metal and carbene character. The 5a antibonding counterpart of this interaction constitutes the LUMO (Lowest Unoccupied Molecular Orbital) of the complex. The 4a HOMO and 3a SHOMO (Second Highest Occupied Molecular Orbital) of 3a are the essentially unperturbed 1a and 2a orbitals of the $\text{CpMn}(\text{CO})_2$ fragment. The carbene lone pair orbital σ is strongly stabilized through donation to the Mn d_{xy} based 4a orbital.

When the carbene ligand is rotated 90° , as in complex 3b, the resultant molecular orbitals of the complex are significantly different: The carbene π^* ligand now interacts with the $\text{CpMn}(\text{CO})_2$ 1a orbital. The resultant strongly stabilized molecular orbital 2a is largely Mn d_{xz} based with contributions from both the $\text{CO}2\pi_x$ and carbene π^* . The 3a molecular orbital is similar to that in complex 3a, a largely Mn d_{yz} - $\text{CO}2\pi_y$ based orbital. The HOMO 4a is essentially the unperturbed 3a non-bonding HOMO of $\text{CpMn}(\text{CO})_2$. The LUMO 5a is a largely carbene π^* based orbital with some contribution from Mn d_{xz} and $\text{CO}2\pi_x$. A diagrammatic comparison of the carbene π^* - $\text{CpMn}(\text{CO})_2$ interactions for complexes 3a and 3b is given in Fig. 5. The contour plots given in Fig. 6 illustrate the C1 localized nature of the LUMO. The composition of the molecular orbitals of 3a and 3b are summarized in Tables 1 and 2.

The Mulliken populations listed in Table 3 indicate that both the σ and π interactions of the carbene ligand with Mn are slightly weakened in complex 3b relative to 3a. It is noted that backdonation to the $\text{CO}2\pi$ is reduced by 0.04 in 3b relative to 3a due to competition between CO and the carbene for bonding with the Mn d_{xz} orbital.

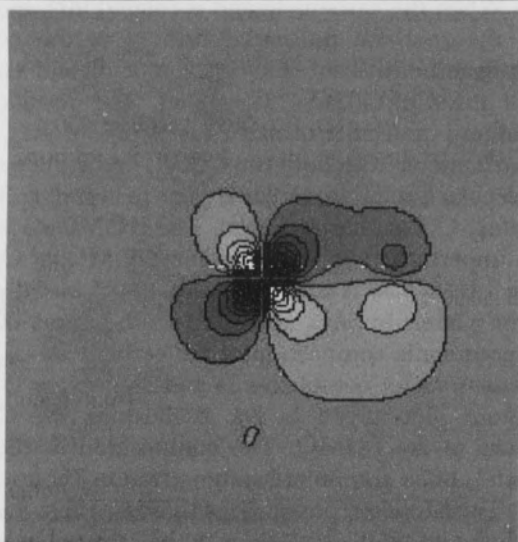
The overlap integral between the carbene π^* and $\text{CpMn}(\text{CO})_2$ 3a in 3a is 0.117. The overlap between carbene π^* and $\text{CpMn}(\text{CO})_2$ 1a in 3b is 0.116. The carbene σ - $\text{CpMn}(\text{CO})_2$ 4a overlap integrals in 3a and 3b are 0.309 and 0.304, respectively. Clearly the difference in stability of the two conformers cannot be attributed to changes in frontier orbital overlap on rotation.

The energies of the frontier molecular orbitals of 3a and 3b are given in Table 4. The average energy of the occupied metal based orbitals is relatively unchanged upon rotation of the carbene ligand (-5.78eV and -5.58eV for 3a and 3b, respectively). This indicates that stability lost by elimination of the carbene π^* - 3a interaction is approximately countered

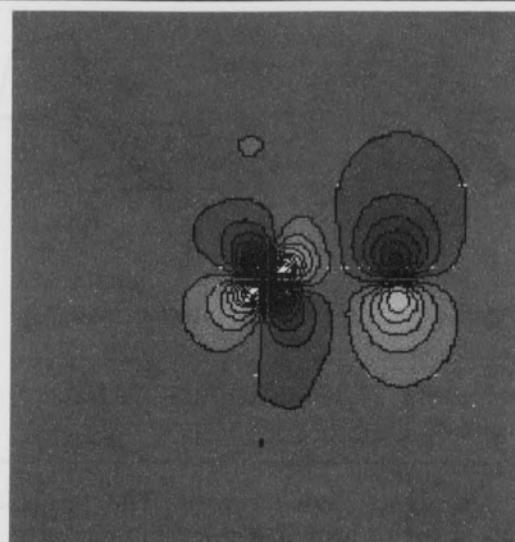
Table 1: Percent character of valence MOs of complex 3a.

	THOMO	SHOMO	HOMO	LUMO	SLUMO	TLUMO
Energy (eV)	-6.12	-5.85	-5.35	-1.58	0.01	0.14
% Mn	63.7	80.0	80.3	45.8	62.1	61.1
%Mn 3d	62.2	76.4	77.9	43.9	53.5	47.6
% Cp (e_1'')	****	****	2.2	5.5	10.6	13.0
%CO 2π	****	18.0	13.9	****	11.2	13.0
% CB lp	****	****	****	****	2.3	****
% CB pz	31.6	****	****	46.6	8.8	6.6

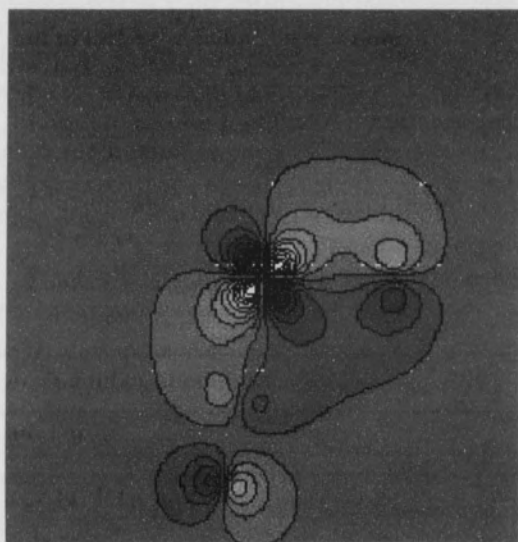
Fenske-Hall Approximate Molecular Orbital Analysis of the Chelating Carbene Complex
 $\eta^5\text{-Cp}^*(\text{CO})\text{Mn}\{\text{C}(\text{OEt})\text{CH}_2\text{PPh}_2\}$



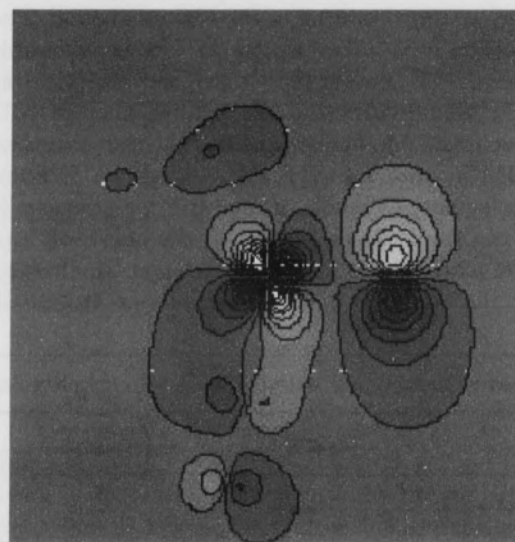
Complex 3a HOMO



Complex 3a LUMO



Complex 3b THOMO



Complex 3b LUMO

Fig. 6. Contour plots of the metal carbene π bonding and antibonding interactions in complexes 3a and 3b.

by that gained by the introduction of the carbene π^* -1a interaction on going from 3a to 3b. Such a result is consistent with ligand additivity models such as that of Bursten and Green (1988). The principal factor to which we

attribute the stability of 3a over 3b is the difference in HOMO energy between the complexes. In complex 3a, the orbital stabilized by the π^* of the carbene ligand is the 3a non-bonding HOMO of the $\text{CpMn}(\text{CO})_2$ fragment. This

John P. Graham

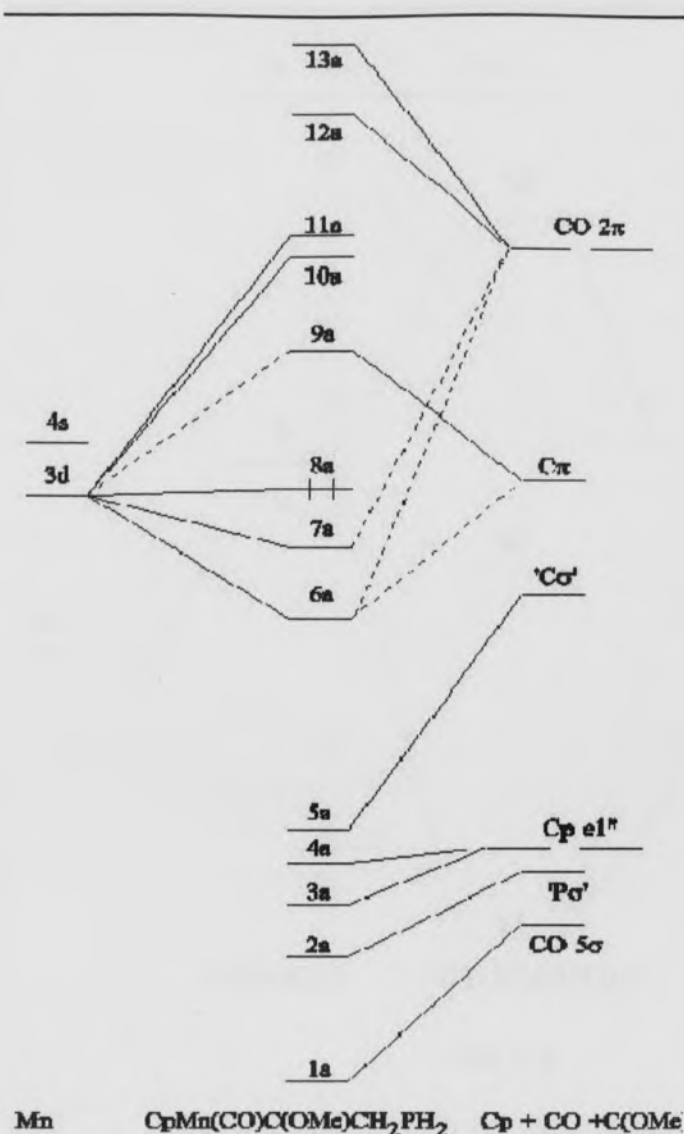


Fig. 7. A molecular orbital description of complex 1a.

results in a HOMO for complex 3a which is a Mn-CO 2π stabilized orbital. In complex 3b, the carbene π^* interacts with the already CO stabilized CpMn(CO) $_2$ 1a orbital, leaving a non-bonding 3a orbital as the HOMO of the complex while further stabilizing the THOMO (Third Highest Occupied Molecular Orbital). It is well known (Pearson, 1987) that the stability of organometallic complexes can be related to the magnitude of the energy difference between the HOMO and LUMO (HOMO-LUMO gap). Complex 3a has a calculated HOMO-LUMO gap of 3.77eV, considerably higher than that of complex 3b (2.91eV). As the LUMO energies in each complex are similar, this effect can be attributed mainly to the metal -

carbene bonding π^* interactions. These observations are consistent with those in Fenske's and Kostic's (1982) account of the importance of non-bonding and antibonding molecular orbitals in the stereochemistry of organometallic complexes.

Comparison of the model complexes 1a and 3.--A molecular orbital diagram for the chelating complex 1a, given as the interaction between the fragments Mn, CO, Cp, and C(OMe)CH $_2$ PH $_2$ is given in Fig. 7. The composition of the molecular orbitals is summarized in Table 5. The largely metal based 6a, 7a, and 8a orbitals are similar in energy and composition to the analogous 2a, 3a, and 4a orbitals of 3b. The HOMO-LUMO gap in complex is 2.63eV. The Mulliken population of the CO 2π orbitals in 1a is also similar to that in 3b. The most distinct difference in the molecular orbital diagrams of 1a and 3b is the energy of the C σ fragment orbital of the carbene ligand. In complex 3b, the C σ orbital is found at -7.91eV compared to -6.28eV in 1a. This increased basicity of the carbene C lone pair arises from a C1-P interaction in the chelating ligand and is discussed below. The Mulliken population of the 'C σ ' orbital in 1a is considerably lower than that in 3b, which also reflects the increased donor ability of the ligand. The carbene π^* Mulliken population in the chelating ligand is considerably higher than that in 3a or 3b. We suggest this increase in backdonation to the carbene ligand is a result of the increased electron density at the metal center due to the more basic C σ orbital. Despite these differences, the most interesting features of the molecular orbital diagram (the largely metal based orbital energies and compositions) are very similar to those of complex 3b. This suggests that the observed differences in properties of complexes 1 and 3 arise largely from the orientation of the carbene ligand.

A molecular orbital diagram of the chelating carbene ligand C(OMe)CH $_2$ PH $_2$, depicted as the interaction of C(OMe)CH $_2$ and PH $_2$ fragments, is presented Fig. 8. The picture on the right shows the ligand with the C-C-P angle the same as in complex 1 (89 $^\circ$). The left-hand picture shows the ligand with a C-C-P angle relaxed to 109 $^\circ$. In each case the 1a' orbital is clearly the CH $_2$ -PH $_2$ bond. When $\theta = 109^\circ$, we see that the 2a' and 3a' orbitals are essentially unperturbed P and C1 lone pairs respectively. When $\theta = 89^\circ$, the P and C1 lone pairs are brought closer together, resulting in a filled-filled interaction. The resulting molecular orbitals, 2a' and 3a', have considerable C1 and P character. The 2a' orbital is more localized on the P atom and slightly lower in energy than the corresponding 2a' orbital at 109 $^\circ$. The 3a' molecular orbital, the C1-P antibonding combination, is considerably destabilized and largely localized on the C1 atom. The 1a' LUMO in each case is the C-O antibonding π orbital of the carbene fragment. The net effect of closing the C-C-P angle is the formation of a strongly basic frontier orbital, C1-P

Fenske-Hall Approximate Molecular Orbital Analysis of the Chelating Carbene Complex
 $\eta^5\text{-Cp}'(\text{CO})\text{Mn}\{\text{C}(\text{OEt})\text{CH}_2\text{PPh}_2\}$

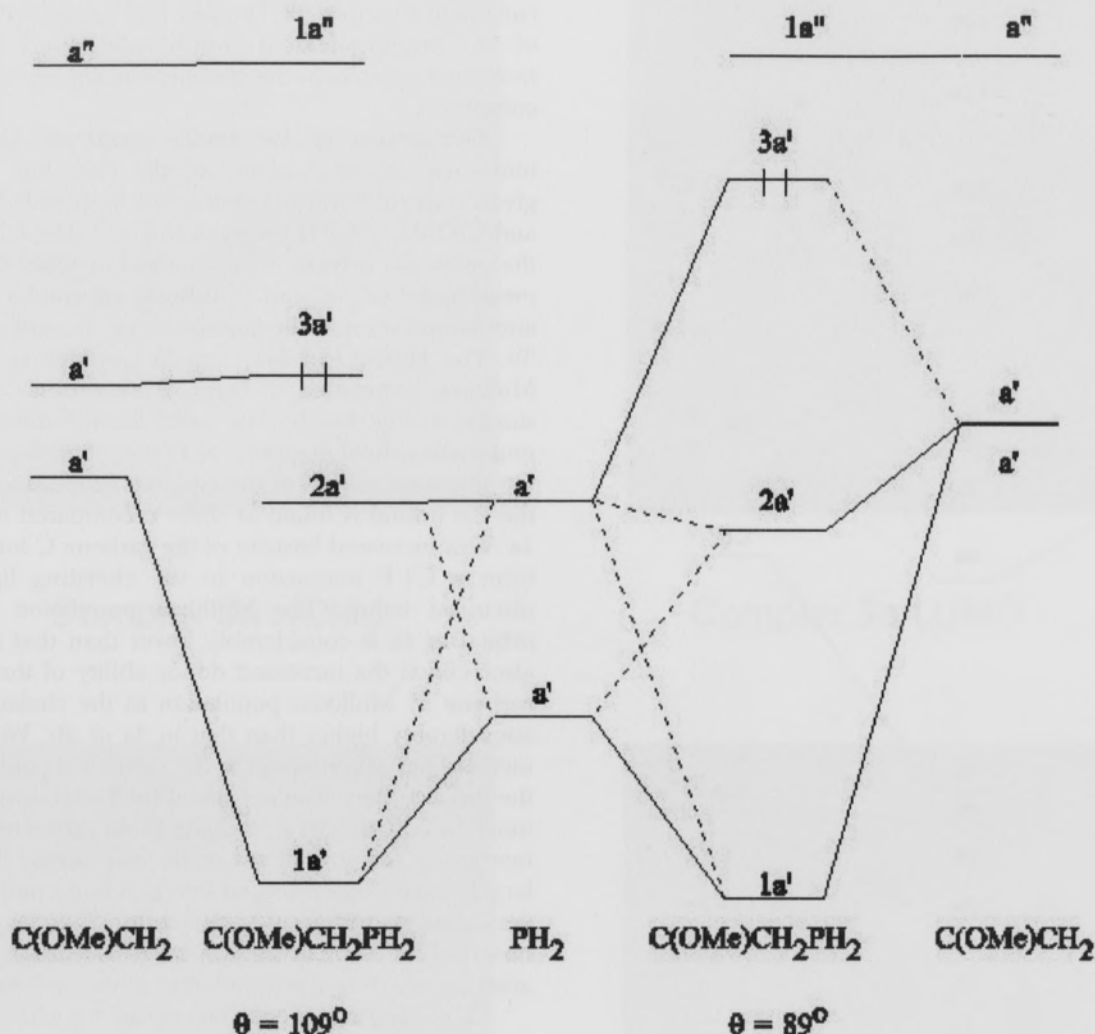


Fig. 8. A molecular orbital description of the chelating ligand $\text{C}(\text{OMe})\text{CH}_2\text{PH}_2$ at $\theta = 89^\circ$ and 109° .

antibonding in nature, more heavily localized on C1. This accounts for the enhanced basicity observed in the molecular orbital diagram of 1a.

The nonbonding HOMO of complex 1a should result in an increased oxidation potential relative to complex 3a. We would also expect a reversible 2e oxidation process in 1a. Indeed, the oxidation potential of 1 has been determined to be 0.54V greater than that for 3. It has been observed that the oxidation potential for Mn(I) complexes changes approximately half as fast as the HOMO energy (Lichtenberger and Fenske, 1976). The difference in HOMO energies between 1a and 3a (1.09eV) is remarkably consistent with this trend. We would expect to see a red-shift

in ligand field transition energies for 1 relative to 3 because of the difference in HOMO-LUMO gaps in model complexes 1a and 3a. This is consistent with experimental data also. The C-O stretching frequency observed in 1 is 43cm^{-1} lower than that found in 3. Correlation with the C-O force constant and $\text{CO}2\pi$ and 5σ Mulliken populations had been shown (Hall and Fenske, 1972) to follow the form

$$k_{\text{CO}} = a(5\sigma) + b(2\pi) + c.$$

Donation from the CO 5σ orbital strengthens the C-O bond, and π backbonding to the $\text{CO}2\pi$ weakens the bond. The 5σ populations in complexes 1a, 3a, and 3b are

John P. Graham

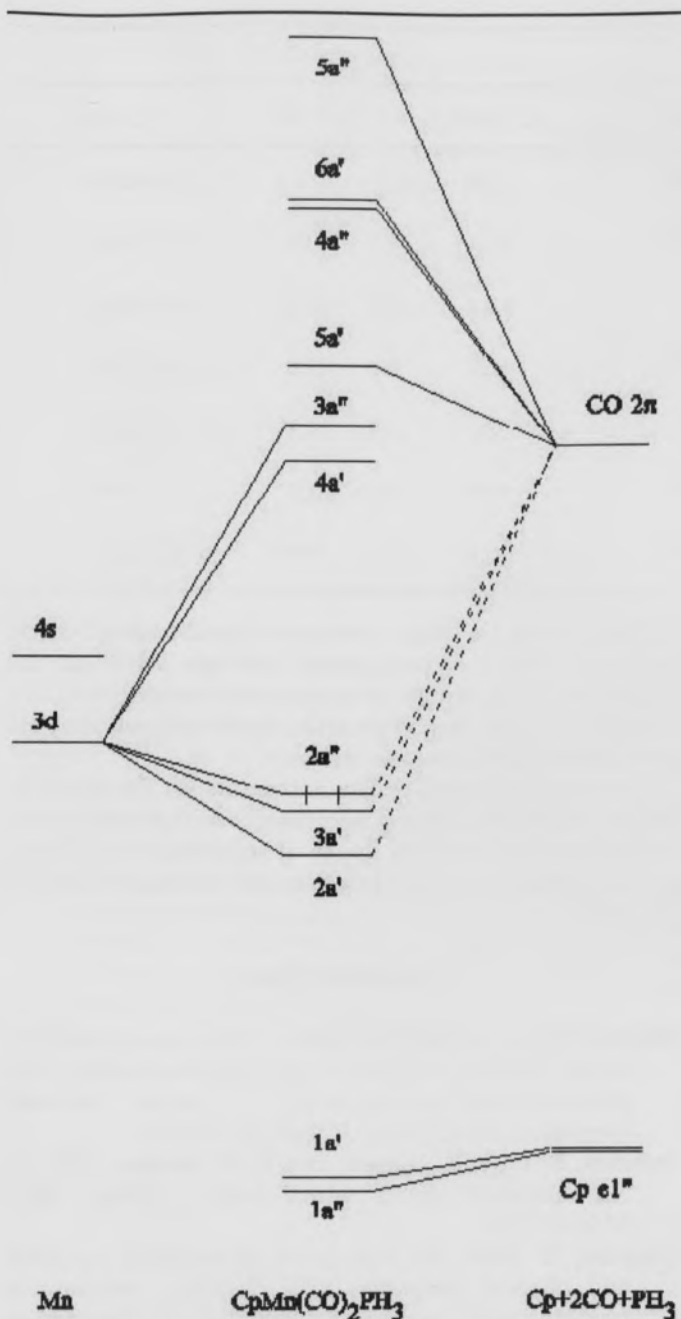


Fig. 9. A molecular orbital description of complex 2a.

essentially invariant. Hence, we would expect the increase in CO 2π population of 1a relative to 3a (+0.037) to give rise to a lower C-O stretching frequency, as experimentally observed. The magnitude of this change in $\nu(\text{CO})$ is difficult to estimate, but it should also be noted that the presence in Cp' in complex 1 vs. Cp in complex 3 would also be expected to contribute to lowering $\nu(\text{CO})$.

Reactivity.--In the presence of CO, complex 1 undergoes a carbene insertion reaction to give the three legged piano stool complex 2. The reaction involves the breaking and formation of several bonds and would be difficult to address using molecular orbital analysis without access to detailed mechanistic information. A molecular orbital description for the model complex 2a, $\text{CpMn}(\text{CO})_2(\text{PH}_3)$, is given in Fig. 9. The molecule is represented by the interaction of CpMn, $2\times\text{CO}$, and PH_3 fragments. All three metal based $d\pi$ orbitals are stabilized through interaction with the CO ligands. The resultant HOMO is bonding, and the pattern of $d\pi$ based MO's resembles that in the complex 3a (favorable carbene orientation). Factors that we would expect to contribute to the enhanced reactivity of 1a over 3a include the nonbonding nature of the HOMO in 1a and the ring-strain within the carbene ligand (and resultant filled-filled interaction between the carbene C1 and P). The LUMO of 1a is the carbene - Mn π antibonding orbital. Frontier orbital controlled nucleophilic attack on complex 1a would be expected to occur at the carbene C atom (which gives the larger contribution to the LUMO). Hence donation from CO to the LUMO would be expected to weaken the Mn-carbene bond. However the LUMO of complex 3a is also carbene-Mn π -antibonding and is of similar energy. As CO attack is not observed in 3, the nature of the LUMO alone is insufficient to explain the difference in reactivity. However, upon nucleophilic attack at the Mn-carbene antibonding LUMO, Mn-carbene bond cleavage may be facilitated by the ring strain and C1-P interaction within the chelating ligand of 1. Although apparently not the most important differentiating factor in the electrochemistry or spectroscopic properties of 1 and 3, it appears that this ring strain and C1-P antibonding interaction within the chelating carbene ligand may contribute significantly to the observed reactivity of 1. Higher level calculations are currently underway to further study possible mechanisms of nucleophilic attack on complex 1.

Conclusions

The molecular orbital analysis of complexes 3a, 3b, and 1a suggests that the conformational preferences of carbene ligands in complexes of the form $\text{CpMLL}'\text{CB}$, where L and L' differ significantly in π acceptor ability, arises from the presence of a non-bonding HOMO in the 'perpendicular' conformation. There are no significant differences in overlap between the carbene and metal fragment in the two model isomers of 3. The metal based orbitals in 1a may be modeled satisfactorily using complex 3b. From comparisons of the bonding in 3a and 3b, electrochemical and spectroscopic differences between 1 and 3 can be explained. The principal difference between complexes 1a and 3b lies

Fenske-Hall Approximate Molecular Orbital Analysis of the Chelating Carbene Complex
 $\eta^5\text{-Cp}'(\text{CO})\text{Mn}\{\text{C}(\text{OEt})\text{CH}_2\text{PPh}_2\}$

Table 2: Percent character of valence MOs of complex 3b.

	THOMO	SHOMO	HOMO	LUMO	SLUMO	TLUMO
Energy (eV)	-6.70	-5.49	-4.48	-1.58	-0.24	0.45
% Mn	51.7	78.4	94.9	35.4	71.6	58.1
%Mn 3d	49.5	76.5	93.2	33.4	63.2	44.5
% Cp (e_1'')	****	****	****	8.5	13.7	7.6
%CO 2 π	14.2	16.4	****	5.4	8.3	21.8
% CB 1.p.	****	****	****	****	1.7	****
% CB p_z	31.0	1.0	****	50.8	****	6.7

Table 3: Mulliken populations of frontier ligand fragment orbitals in complexes 3a, 3b, and 1a.

	Complex 3a	Complex 3b	Complex 1a
Carbene σ	1.353	1.369	1.200
Carbene π^*	0.706	0.683	0.756
CO 2 π	0.783	0.743	0.750
CO 5 σ	1.420	1.421	1.420

Table 4: Frontier MO energies for complexes 1a, 3a and 3b.

	Complex 3a	Complex 3b	Complex 1a
LUMO	-1.58	-1.59	-1.63
HOMO	-5.35	-4.50	-4.26
SHOMO	-5.86	-5.52	-5.37
THOMO	-6.12	-6.73	-6.69

in the interactions within the chelating ligand of 1a. It is suggested that the filled-filled P-C1 interaction in the chelating ligand, along with the considerable ring strain, contributes to the enhanced reactivity of 1 over 3. The LUMO of 1a, a spatially localized and energetically isolated orbital, is an ideal site for nucleophilic attack. Attack at the

LUMO, which is Mn - carbene π antibonding, would encourage Mn - carbene bond cleavage. Although the LUMO of 3a is similar in energy and composition, it is suggested that the ring strain in the chelating ligand may aid Mn-carbene bond cleavage in 1.

ACKNOWLEDGMENTS.—The author thanks Dr. Bruce E. Bursten of the Ohio State University for his valuable advice and insights and Dr. Noel Lugan of Laboratoire de Chimie de Coordination for providing data and creating the basis of this study.

Literature Cited

- Bursten, B. E., and M. R. Green.** 1988. Ligand additivity in the vibrational spectroscopy, electrochemistry and photoelectron spectroscopy of metal carbonyl derivatives. *Prog. Inorg. Chem.* 36:393-485.
- Bursten, B. E., J. R. Jensen, and R. F. Fenske.** 1978. An $X\alpha$ optimized atomic orbital basis. *J. Chem. Phys.* 68:3320-3321.
- Clayton, T.** 1989. The correlation of structure, reactivity and physical properties with electronic structure in transition metal complexes. Unpubl. Ph.D. Dissertation. The Ohio State University, Columbus, OH.
- Fenske, R. F., and N. M. Kostic.** 1982. Criteria of maximum overlap and minimum orbital energy in molecular orbital studies of conformations of transition-metal carbene and carbyne complexes. *J. Am. Chem. Soc.* 104:3879-3884.
- Frenking, G., and N. Froelich.** 2000. The nature of bonding in transition metal compounds. *Chem. Rev.* 100:717-774.
- Hall, M. B., and R. F. Fenske.** 1972. Electronic structure and bonding in methyl- and perfluoromethyl-

John P. Graham

Table 5: Percent character of valence MOs of complex 3a.

	THOMO	SHOMO	HOMO	LUMO	SLUMO	TLUMO
Energy (eV)	-6.69	-5.37	-4.26	-1.63	0.16	0.55
% Mn	48.9	76.4	96.5	37.0	67.0	59.7
%Mn 3d	46.6	74.4	95.0	35.3	57.2	45.7
% Cp (e_1'')	****	****	****	7.3	12.9	8.1
%CO 2π	13.4	17.3	****	5.8	14.0	20.8
% CB 'lp'	****	****	****	****	4.7	****
% CB p_z	34.7	1.0	****	49.0	****	5.9

(pentacarbonyl)manganese. *Inorg. Chem.* 11:768-775.

Hall, M. B., and R. F. Fenske. 1972. Force constants and the electronic structure of carbonyl groups. d^6 carbonyl halides and dihalides. *Inorg. Chem.* 11:1619-1624.

Hehre W. J., R. F. Stewart, and J. A. Pople. 1969. Self-consistent molecular-orbital methods. I. use of gaussian expansions of Slater-type atomic orbitals. *J. Chem. Phys.* 51:2657-2665.

Kiel, W. A., L. Gong-Yu, and J. A. Gladysz. 1980. Unprecedented regioselectivity and stereospecificity in reactions of $\text{Ph}_3\text{C}^+\text{PF}_6^-$ with rhenium alkyls of the formula $(\eta^5\text{-C}_5\text{H}_5)\text{Re}(\text{NO})(\text{PPh}_3)(\text{CH}_2\text{R})$. *J. Am. Chem. Soc.* 102:3299-3301.

Lichtenberger, D. L., and R. F. Fenske. 1976. The transferability of molecular fragment canonical orbitals. *J. Chem. Phys.* 64:4247-4264

Pearson, R. G. 1987. Recent advances in the concept of hard and soft acids and bases. *J. Chem. Ed.* 64:561-567.

Schilling, B. E. R., R. Hoffmann, and D. L. Lichtenberger. 1979. $\text{CpM}(\text{CO})_2(\text{ligand})$ complexes. *J. Am. Chem. Soc.* 101:585-591.

Schrock, R. R. 2001. Transition metal-carbon multiple bonds. *J. Chem. Soc., Dalton Trans.* 18:2541-2550.